# Hydrophobic Mismatch in Gramicidin A′/Lecithin Systems†

Paula I. Watnick and Sunney I. Chan*

*Arthur Amos Noyes Laboratory of Chemical Physics, California Institute of Technology, Pasadena, California 91125*

Phoebe Dea

*Department of Chemistry and Biochemistry, California State University at Los Angeles, Los Angeles, California 90032*

*Received October 10, 1989; Revised Manuscript Received March 29, 1990*

ABSTRACT: Gramicidin A′ (GA′) has been added to three lipid systems of varying hydrophobic thicknesses: dimyristoyllecithin (DML), dipalmitoyllecithin (DPL), and distearoyllecithin (DSL). The similarity in length between the hydrophobic portion of GA′ and the hydrocarbon chains of the lipid bilayers has been studied by using $^{31}P$ and $^{2}H$ NMR. Hydrophobic mismatch has been found to be most severe in the DML bilayer system and minimal in the case of DSL. In addition, the effects of hydrophobic mismatch on the cooperative properties of the bilayer have been obtained from $^{2}H$ NMR relaxation measurements. The results indicate that incorporation of the peptide into the bilayer disrupts the cooperative director fluctuations characteristic of pure multilamellar lipid dispersions. Finally, the GA′/lecithin ratio at which the well-known transformation from bilayer to reverse hexagonal ($H_{II}$) phase occurs (Van Echteld et al., 1982; Chupin et al., 1987) is shown to depend on the acyl chain length of the phospholipid. A rationale is proposed for this chain length dependence.

Gramicidin A′ (GA′) is a mixture of three related linear pentadecapeptides produced by the *Bacillus brevis* bacterium. By binding to RNA polymerase, GA′ is believed to inhibit the transcription of genes involved in vegetative growth (Fisher & Blumenthal, 1982). In lipid bilayers, GA′ forms a transmembrane channel which allows the passage of monovalent cations. Although this function does not appear to be important in vivo, the possibility of using GA′ as a simple model in the study of membrane channels, membrane/protein interactions, and transmembrane $\alpha$-helices has spurred much interest in its membrane-bound conformation.

Evidence indicates that GA′ exists as a single helical dimer in many amphipathic systems (Urry et al., 1971, 1983). NMR studies of isotopically labeled GA′ in DML have shown that most of the C-terminal ends are exposed to the hydrophilic region of the bilayer, while the N-terminal ends are buried in the hydrocarbon region (Weinstein et al., 1979, 1980). This indicates that the N-terminus of the GA′ monomer residues in the hydrophobic region of the bilayer and is probably the point of attachment in dimer formation.

Infrared and Raman spectroscopic investigations of the secondary structure of GA′ in bilayer membranes indicate a $\beta$-sheet hydrogen-bonding pattern (Iqbal & Weidekamm, 1980; Naik & Krimm, 1984, 1986). More recent solid-state NMR studies of GA′/DML bilayers revealed $^{13}C$–$^{13}C$ dipolar couplings in multiply labeled GA′ that are consistent with a single-stranded helix of pitch 6.3 (Cornell et al., 1988a). Modeling studies have shown this $\beta$-helix to be 26–30 Å long with an inner diameter of 4 Å (Veatch et al., 1974). Because several of GA′'s Trp residues are located near the headgroup region of the bilayer, the GA′ has a pronounced cone shape at both ends of the dimer. Alternating D and L amino acids allow all side chains to face the helix exterior, while the more polar carbonyl and amino groups line the interior of the helix. This conformation of GA′ is known as $\beta^{6.3}$.

A transmembrane segment in a protein has hydrophobic and hydrophilic regions which match those of the surrounding lipid bilayer. When the hydrophobic lengths of the transmembrane portion of the protein and the lipid bilayer into which it is reconstituted are not equal, a situation known as hydrophobic mismatch exists. Hydrophobic mismatch has been shown to affect the interaction of many proteins with lipid bilayers (Kusumi & Hyde, 1982; Lewis & Engelman, 1983; Riegler & Moehwald, 1986). Pearson and co-workers have suggested two ways in which the hydrocarbon region of a bilayer may deform to compensate for hydrophobic mismatch (Pearson et al., 1983, 1984). A lipid bilayer may expand by allowing the ratio of trans to gauche bonds in the lipid chains to increase or may shrink by decreasing this ratio. Tilting of the acyl chains in the bilayer toward or away from the bilayer normal also changes the bilayer thickness. Furthermore, an expansion or compression of the hydrophobic region of the bilayer will lead to an increase or decrease in the ratio of the headgroup cross-sectional area ($A_H$) to the hydrocarbon cross-sectional area ($A_C$), respectively.

Adjustments of the bilayer in order to accommodate GA′ have been observed by Raman and infrared spectroscopies (Chapman et al., 1977; Lee et al., 1984; Aslanian et al., 1986). The number of trans conformers in both the DML and DPL hydrocarbon region has been found to increase upon addition of GA′. The induction of reverse hexagonal phase ($H_{II}$) in phosphatidylcholines with acyl chain lengths greater than 16 carbons by GA′ has been widely studied by NMR and X-ray diffraction techniques (Van Echteld et al., 1982; Killian et al., 1986; Chupin et al., 1987). More recently, Killian et al. (1989) have reported that an excess bilayer thickness is a prerequisite for $H_{II}$ phase formation in GA′–phosphatidylcholine model membranes. Various mechanisms have also been proposed to account for the known effects of GA′ on lipid bilayers (Killian

† Contribution No. 8343 of the Division of Chemistry and Chemical Engineering, California Institute of Technology. This work was supported by Grants GM-22432 (S.I.C.), GM-36132 (P.D.), and RR-08101 (P.D.) from the National Institutes of General Medical Sciences, U.S. Public Health Service, and by the donors of the Petroleum Research Fund, administered by the American Chemical Society. P.I.W. was a recipient of a National Research Service Award (T32 GM07616) from the National Institutes of General Medical Sciences.

* To whom correspondence should be addressed.

0006-2960/90/0429-6215$02.50/0 

& De Kruijff, 1988; Cornell et al., 1988b).

In this paper, the effects of hydrophobic mismatch on the physical properties of the lipid bilayer and on the factors leading to $H_{II}$ phase formation in GA′/lecithin systems are studied by using $^{31}P$ and $^{2}H$ NMR. The observed chemical shift anisotropy $\langle\Delta\sigma\rangle$ of the $^{31}P$ NMR powder pattern reflects the motions and orientation of the lipid headgroup. Furthermore, the $\langle\Delta\sigma\rangle$ of $H_{II}$ phase is half that of the bilayer phase and of opposite sign so that these two phases are easily distinguished by $^{31}P$ NMR. The quadrupolar splittings ($\Delta\nu_Q$) observed in the $^{2}H$ NMR spectra of mixtures of GA′ and selectively deuterated lipids should reflect the adjustment of the lipid chains in response to the mismatch between the hydrophobic length of GA′ and the lipid hydrocarbon chains. Finally, the $^{2}H$ NMR relaxation measurements should give an indication of whether the cooperative director fluctuations (Watnick et al., 1987, 1990) are disrupted by incorporation of the peptide into the bilayer membrane.

## Experimental Procedures

*Materials and Methods.* Dimyristoyllecithin (DML), dipalmitoyllecithin (DPL), and distearoyllecithin (DSL) were purchased from Avanti Polar Lipids. GA′ was purchased from Boehringer Mannheim Biochemicals. DML (DML-*9,9′,10,10′-d*$_4$), DPL (DPL-*9,9′,10,10′-d*$_4$), and DSL (DSL-*9,9′,10,10′-d*$_4$) were deuterated at the 9- and 10-positions on both acyl chains as described previously (Watnick et al., 1987).

GA′ was dissolved in methanol and then added to either DML, DPL, or DSL in appropriate amounts. DPL and DSL are not sufficiently soluble in methanol. In order to dissolve these lipids, chloroform was added to the GA′/methanol solution. The organic solvent was evaporated from the GA′/lipid samples under low vacuum until most of the solvent was removed. The sample was then placed under high vacuum overnight. Samples were hydrated in 400 mM Tris and 40 mM NaCl buffer (pH 7.4). All preparations contained less than 20% (w/w) lipid in water. In order to reach an equilibrium distribution of GA′ in the bilayers, it was necessary to incubate the samples 5–8 °C above the thermal phase transition temperature of the mixtures for approximately 12 h. The NMR measurements were performed at 30 °C for the DML, 45 °C for the DPL, and 63 °C for the DSL systems. These temperatures are well above the gel-to-liquid crystalline phase transition temperatures of the respective systems. In addition, variable-temperature $^{31}P$ NMR experiments were carried out on some GA′/phospholipid systems to characterize the lipid structure.

*Instrumentation.* $^{2}H$ NMR experiments were conducted on a Bruker AM 500 spectrometer. The TLO transmitter pulse was attenuated to 1 V peak/peak and used to drive an Amplifier Research 200L amplifier. The amplified pulse was then fed into a home-built high-power deuterium probe. This arrangement provided a 3.5-$\mu$s 90° pulse.

$^{31}P$ NMR spectra were obtained on a Bruker AM 400 spectrometer. A broad-band probe yielding a 10-$\mu$s 75° pulse was used for the acquisition of the spectra. $^{1}H$–$^{31}P$ dipolar couplings were eliminated by gated broad-band proton decoupling at a power of 20 W.

*Pulse Sequences and Data Analysis.* The pulse sequences and methods of data analysis for the relaxation experiments have been described in detail previously (Watnick et al., 1987). The following inversion–recovery pulse sequence, modified to include a terminal quadrupolar echo sequence, was used to measure $T_1$:

$$90^\circ_x\text{–}90^\circ_y\text{–}90^\circ_y\text{–}90^\circ_x\text{–}\tau\text{–}90^\circ_x\text{–}t_1\text{–}90^\circ_y\text{–}t_1\text{–acquire}$$

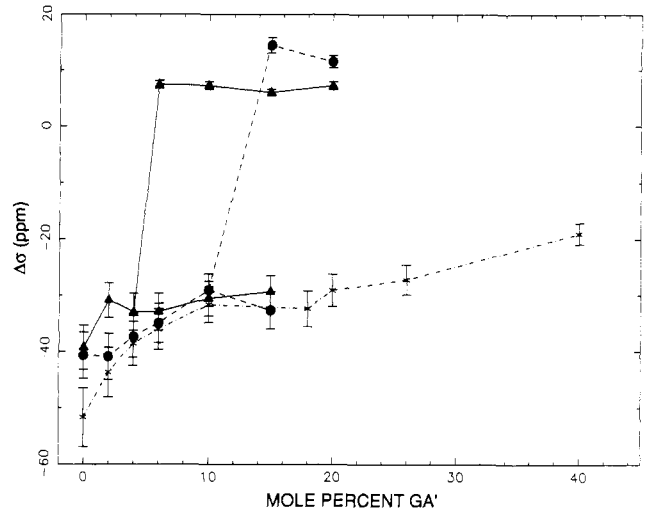


FIGURE 1: Dependence of the $^{31}P$ chemical shift anisotropy values on GA′ concentration for the three lipid systems studied. The $^{31}P$ NMR spectra were recorded at 161.98 MHz, and the measurements were carried out at 30 °C for the DML (×), 45 °C for the DPL (●), and 63 °C for the DSL (▲) systems.

where $\tau$ represents the variable delay and $t_1$ is the fixed quadrupolar echo delay.

$T_{1\rho}$ was measured by using the pulse sequence:

$$90^\circ_x\text{–}(\theta)_y\text{–}t_1\text{–}90^\circ_y\text{–}t_1\text{–acquire}$$

Here, $\theta$ is the variable spin-locking pulse and $t_1$ again represents the quadrupolar echo delay.

$T_2$ was measured by using a simple quadrupolar echo sequence with central 180° pulses included to refocus resonant offset as well as heteronuclear dipolar interactions. This pulse sequence is shown:

$$90^\circ_x\text{–}\tfrac{1}{4}t_1\text{–}180^\circ_x\text{–}\tfrac{1}{4}t_1\text{–}90^\circ_y\text{–}\tfrac{1}{4}t_1\text{–}180^\circ_x\text{–}\tfrac{1}{4}t_1\text{–acquire}$$

where $t_1$ is a variable delay. Data were analyzed by recording the intensity at a 90° singularity of the deuterium powder pattern for each $t_1$ time point. The array of the intensities was then fit to an exponential decay.

## Results

The $^{31}P$ NMR studies of DML, DPL, and DSL bilayers containing GA′ are summarized in Figure 1. Here, the observed $\langle\Delta\sigma\rangle$'s for the various lipids are plotted versus the mole percent GA′. In each of the three lipid systems studied, the observed $^{31}P$ chemical shift anisotropy of the bilayer decreases upon addition of GA′. The discontinuities observed in the $\langle\Delta\sigma\rangle$ above 10 mol % GA′ in DPL and 4 mol % GA′ in DSL reflect a transition from bilayer to $H_{II}$ phase. This is characterized by a more than 2-fold reduction in $\langle\Delta\sigma\rangle$ for the $H_{II}$ phase, indicating increased motional freedom of the phospholipid headgroup. DML is found to remain in the bilayer phase even at very high GA′ concentrations; $\langle\Delta\sigma\rangle$, however, is significantly reduced at the higher GA′ concentrations, similar to results reported by Cornell et al. (1988b).

Figure 2 shows the dependence of $\Delta\nu_Q$ on GA′ concentrations for the 9- and 10-deuterons in DML-*9,9′,10,10′-d*$_4$, DPL-*9,9′,10,10′-d*$_4$, and DSL-*9,9′,10,10′-d*$_4$. For GA′/DML, $\Delta\nu_Q$ increases by approximately 6 KHz as the concentration of GA′ in the bilayer is increased to 6 mol %. These results are comparable to those reported by Rice and Oldfield for this system (Rice & Oldfield, 1979). An increase of 3 kHz is observed over the same concentration range for DPL. In the case of DSL, $\Delta\nu_Q$ remains constant within experimental error up through a GA′ concentration of 8 mol %. The presence

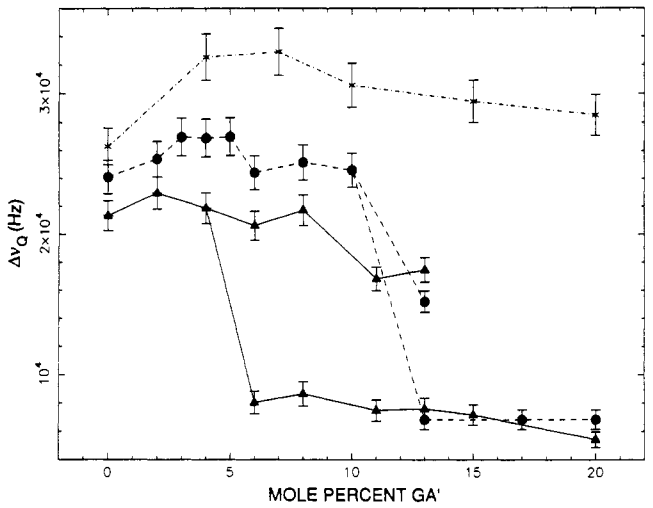


FIGURE 2: Dependence of the deuterium quadrupolar splitting on GA' concentration. The $^2$H NMR spectra were recorded at 76.77 MHz, and measurements were carried out at 30 °C for the DML (×), 45 °C for the DPL (●), and 63 °C for the DSL (▲) systems.

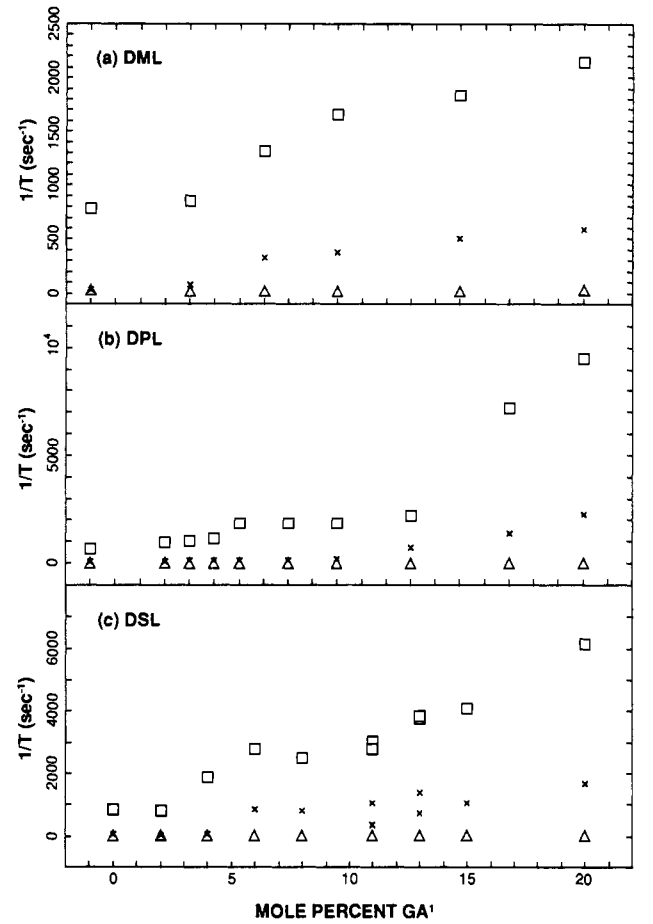


FIGURE 3: $T_1^{-1}$, $T_{1\rho}^{-1}$, and $T_2^{-1}$ for various concentrations of GA' in (a) DML, (b) DPL, and (c) DSL systems. See text for the details of the NMR relaxation measurements. An experimental error of 10% was obtained. The following symbols are used for the relaxation times: (△) $T_1^{-1}$, (×) $T_{1\rho}^{-1}$, and (□) $T_2^{-1}$.

of $H_{II}$ components in DPL and DSL accounts for the discontinuities in $\Delta\nu_Q$ at 10 and 4 mol % GA', respectively. Lipids in the bilayer and $H_{II}$ phases are in slow exchange on the time scale of these experiments, and the observed spectra correspond to a superposition of the component spectra.

In Figure 3, the dependences of the relaxation rates $T_1^{-1}$, $T_{1\rho}^{-1}$, and $T_2^{-1}$, for the 9- and 10-deuterons on the hydrocarbon

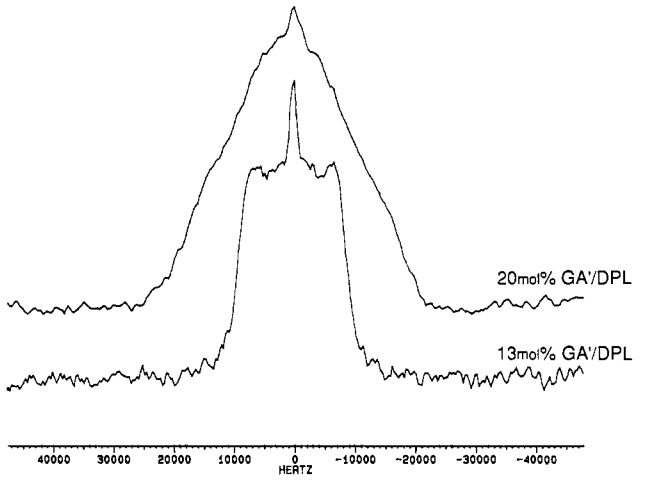


FIGURE 4: 76.77-MHz $^2$H NMR spectra of (a) 20 mol % and (b) 13 mol % GA' in DPL at 45 °C.

chains of DML, DPL, and DSL are depicted as a function of GA' concentration. For all three lipid systems, $T_1^{-1}$ is significantly less than $T_{1\rho}^{-1}$ and $T_2^{-1}$. The presence of $H_{II}$ phase in the GA'/DPL and GA'/DSL systems causes $T_{1\rho}^{-1}$ and $T_2^{-1}$ to increase dramatically with increasing GA' concentration. The $T_1^{-1}$'s of the bilayers are not sensitive to the incorporation of GA' and are quite similar for the three lipid systems. Upon addition of GA', only the $T_{1\rho}^{-1}$ of the DML bilayer increases dramatically. On the other hand, the $T_2^{-1}$'s of the bilayer systems are strongly dependent upon the GA' concentration, and the enhancement in the relaxation rates is comparable for all three lipid systems. These results indicate that addition of GA' to all three bilayers enhances slow motions, but in the case of DML, the motions affected extend to the megahertz regime.

When additional GA' is added to the $H_{II}$ phases of both GA'/DPL and GA'/DSL, an abrupt increase is observed in the $T_2^{-1}$ of deuterons at the 9- and 10-positions of the lipid hydrocarbon chains. This dramatic increase in $T_2^{-1}$ is manifested in the line widths of the corresponding one-dimensional $^2$H NMR spectrum. Figure 4 compares the $^2$H NMR spectra of DPL-*9,9',10,10'-d*$_4$ containing 13 and 20 mol % GA'. The small $\Delta\nu_Q$ observed in both the 13 and 20 mol % GA' spectra merely reflects the dominant contribution to the spectra from lipids in the $H_{II}$ phase. However, the line width of the 20 mol % GA' spectrum is significantly greater than that of the 13 mol % spectrum. This indicates that the slow motions of the lipid hydrocarbon chains in the $H_{II}$ phase increase with increasing GA' concentration.

To ascertain whether the motions of the headgroups are affected in a similar manner, the line widths of the $H_{II}$-phase $^{31}$P NMR spectra of GA'/DPL recombinants at 15 and 20 mol % GA' are compared in Figure 5. The singularity observed at 7.8 ppm corresponds to the $H_{II}$ phase. The line widths of the $^{31}$P NMR spectra at 15 and 20 mol % GA' are remarkably similar. This suggests that, although addition of GA' to the $H_{II}$ phase significantly enhances slow motions in the lipid hydrocarbon chains, any corresponding slow motions in the lipid headgroups are not comparably affected.

## Discussion

*Hydrophobic Mismatch in GA'/Lecithin Bilayer Systems.* Hydrophobic mismatch in GA'/lecithin bilayers has been studied by $^{31}$P NMR and $^2$H NMR. The lipids DML, DPL, and DSL have identical headgroups, but their acyl chain lengths differ. $^{31}$P NMR showed that $\langle\Delta\sigma\rangle$ decreases uniformly as GA' is incorporated into each of these three bilayers.

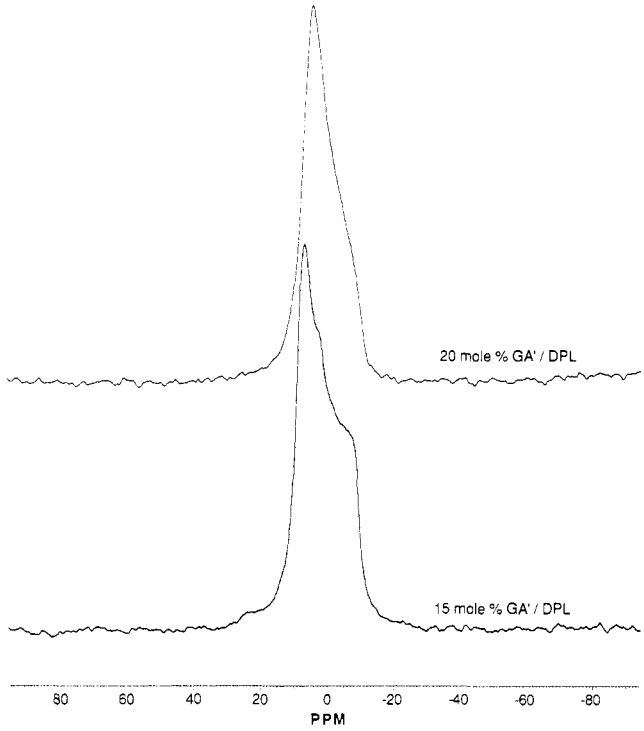


FIGURE 5: 161.98-MHz $^{31}P$ NMR spectra of (a) 20 mol % and (b) 15 mol % GA′ in DPL at 45 °C.

In contrast, the deuterium order parameter of the C–D bond at the 9- and 10-positions of both acyl chains measured from the $^2H$ NMR spectra of specifically deuterated lipids in the bilayer phase exhibits changes characteristic of each lipid. As GA′ is added to the respective bilayers, the deuteron quadrupolar splitting increases the most for DML, increases somewhat for DPL, and remains essentially unchanged for DSL. These results indicate that GA′ interacts in a similar manner with the headgroups of all the phospholipid bilayers under consideration here but perturbs the hydrocarbon chains of each bilayer to a varying degree.

$\Delta\nu_Q$ is related to $\beta'$, the angle between the C–D bond vector and the director through the order parameter $S_{CD} = \langle(1/2)(3 \times \cos^2 \beta' - 1)\rangle$ (Seelig, 1977):

$$\Delta\nu_Q = \frac{3}{4}\frac{e^2qQ}{\hbar}|\langle(1/2)(3\cos^2\beta' - 1)\rangle| \qquad (1)$$

A change in the order parameter $S_{CD}$ upon the addition of GA′ may be attributed to a change in the average orientation of the chain segment with respect to the director. In pure lipid bilayers, the "average" angle between the hydrocarbon chain segment and the director for a methylene carbon has been shown to be approximately 70°. If the acyl chain adopts conformations that increase this angle for the $CD_2$ segment in question, $\Delta\nu_Q$ will increase. We surmise, therefore, that the addition of GA′ to the three lipid bilayer systems increases the "average" angle $\beta'$ for the C–D bond at the 9- and 10-positions by varying amounts. Because the value of $\beta'$ is smaller for a gauche conformer than for a trans conformer, an increase in the "average" $\beta'$ corresponds to an increase in the population of trans conformers at the 9- and 10-positions of the hydrocarbon chain if only gauche and trans conformers contribute to the distribution function. One may conclude, therefore, that the population of trans conformers in this region of the bilayer increases as GA′ is added to DML and DPL. This is consistent with Raman and IR spectroscopic findings (Chapman et al., 1977; Lee et al., 1984; Aslanian et al., 1986). Since no increase in $\Delta\nu_Q$ was observed in the GA′/DSL system, the ratio of trans to gauche conformers must remain essentially constant as GA′ is added to DSL, implying that no hydrophobic mismatch exists for this lipid system.

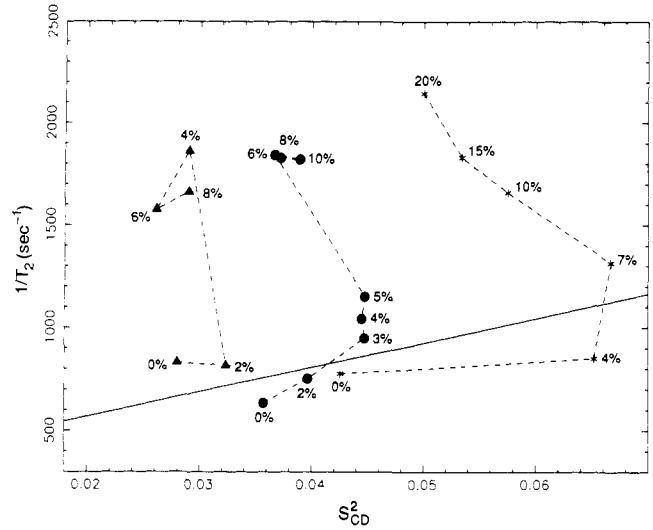


FIGURE 6: A plot of $T_2^{-1}$ versus $S_{CD}^2$ for several concentrations of GA′. Each point is identified with a stoichiometric GA′ concentration for the lipid system: (×) GA′ in DML, (●) GA′ in DPL, and (▲) GA′ in DSL. The best fit line for the [$^2H_{54}$]DML data is included for comparison (Watnick et al., 1990).

If the hydrophobic length of the lipid bilayer is less than that of the added peptide, an increase in the trans conformers of the lipid hydrocarbon region will compensate for the hydrophobic mismatch between a peptide and a lipid bilayer. The results of the $\Delta\nu_Q$ measurements, therefore, indicate that the hydrophobic length of GA′ is longer than that of DML and DPL and is nearly equal to that of DSL. The hydrophobic lengths of pure DML, DPL, and DSL bilayers in the liquid-crystalline phase have been shown to be 27.9, 29.3, and 30.6 Å, respectively (Lewis & Engelman, 1983). Modeling studies have shown the length of the $\beta^{6.3}$ GA′ dimer to be between 26 and 30 Å. A comparison of the hydrophobic lengths of the three lipid bilayers suggests that the hydrophobic length of GA′ is closer to 30 Å, and thus most if not all of the GA′ molecule prefers a hydrophobic environment.

As GA′ is added to the bilayer phase of each GA′/lipid mixture, both the deuterium order parameter as well as the $T_2^{-1}$ of the deuterated lipid varies. As discussed in our recent publication (Watnick et al., 1990), the contribution of cooperative fluctuations to $T_2^{-1}$ takes the form:

$$T_2^{-1}\ (\text{cooperative fluctuations}) \propto \langle\sin^2(2\beta)\rangle S_{CD}^2 \int_{-\infty}^{\infty} \langle\delta\beta(0)\ \delta\beta(\tau)\rangle\ d\tau \qquad (2)$$

where $\beta$ is the angle between the bilayer director and the external magnetic field, $\delta\beta$ is the angle between the average director and the instantaneous director, $\langle\delta\beta(0)\ \delta\beta(\tau)\rangle$ is the correlation function for director fluctuations, and the quantity $\langle\sin^2 2\beta\rangle$ is averaged over a range of $\beta$'s to account for lateral diffusion of the lipid molecules during the time scale of the NMR observation. In bilayer systems where the extent of cooperative motion is similar, a plot of $T_2^{-1}$ versus $S_{CD}^2$ should yield a straight line. If a plot of $T_2^{-1}$ versus $S_{CD}^2$ does not yield a straight line, then the correlation function for director fluctuations must be different in the systems under study. In Figure 6, the $^2H$ NMR $T_2^{-1}$'s of DML-*9,9′,10,10′-d*$_4$, and DSL-*9,9′,10,10′-d*$_4$ bilayers containing varying concentrations of GA′ are plotted versus $S_{CD}^2$. The straight line obtained by plotting $T_2^{-1}$ versus $S_{CD}^2$ for deuterons along the hydrocarbon

chain of a perdeuterated DML lipid bilayer is included for comparison (Watnick et al., 1990). A linear dependence of $T_2^{-1}$ on $S_{CD}^2$ is not observed for any of the GA'/lipid bilayer systems studied. Such large changes in $T_2^{-1}$ cannot be accounted for by changes in the range of lateral diffusion during $T_2$. Upon addition of GA', therefore, motions in each of the bilayers are grossly affected. Furthermore, the motions become very different from those of the pure lipid bilayer.

By use of the continuum theory of nematics, a more detailed description of the effect of hydrophobic mismatch on cooperative fluctuations may be obtained. The expression for the correlation function associated with director fluctuations within the approximation is given by (Pace & Chan, 1982a,b)

$$\langle \delta\beta(0)\, \delta\beta(\tau)\rangle = \sum_{\alpha=1}^{2} \int_{q_\perp^l}^{q_\perp^u} \int_{q_\parallel^l}^{q_\parallel^u} \frac{k_B T \exp(-\tau/\tau_\alpha(q))}{k_{33} q_\parallel^2 + k_{\alpha\alpha} q_\perp^2} 2\pi\, dq_\parallel\, q_\perp\, dq_\perp \quad (3)$$

where $[\tau_\alpha(q)]$ denotes the correlation times associated with the decays of the cooperative distortion:

$$[\tau_\alpha(q)]^{-1} = (k_{\alpha\alpha} q_\perp^2 + k_{33} q_\parallel^2)/\eta_\alpha \quad (4)$$

$k_{11}$, $k_{22}$, and $k_{33}$ are the elastic constants associated with splay, twist, and bend distortions, respectively, $\eta_\alpha$, the effective microviscosities, and $q = 2\pi/\lambda$, where $\lambda$ is the correlation length for a distortion. $\lambda_\perp^u$ and $\lambda_\perp^l$ are the maximum and minimum correlation lengths found in splay and twist bilayer deformations. $\lambda_\parallel^u$ and $\lambda_\parallel^l$ are the corresponding values for the bend deformation. Generally, it is assumed that $k_{11} = k_{22} = (k_{11},k_{22})$ and $k_{33}$ small.

As described previously (Watnick et al., 1987), eq 3 may be used to estimate the order of magnitude of $(k_{11},k_{22})$ and $\lambda_\perp^u$ given the $T_{1\rho}^{-1}$ and $T_2^{-1}$ measurements. Such calculations have been carried out for DML, DPL, and DSL bilayers containing varying concentrations of GA'. The qualitative results are summarized in Figure 7. In Figure 7a, the resulting elastic constants for these three bilayer systems have been plotted versus mol % GA'. In pure lipid bilayers, the $(k_{11},k_{22})$ of DML is much higher than those of DPL and DSL. As GA' is added to each of the bilayers, however, their elastic constants become more similar.

In Figure 7b, the $\lambda_\perp^u$'s of the three lipid systems are graphed as a function of GA' concentration. In the pure bilayers, the $\lambda_\perp^u$ of DML is greater than that of DPL and DSL. As GA' is added to the bilayers, however, $\lambda_\perp^u$ decreases as expected, but $\lambda_\perp^u$ of DML decreases much more rapidly than that of DPL or DSL. Consequently, at high concentrations of GA', $\lambda_\perp^u$ for the DML bilayer is the shortest of the three measured, the $\lambda_\perp^u$ of DPL is intermediate, and the DSL bilayer has the longest $\lambda_\perp^u$.

The difference in the decrease of $\lambda_\perp^u$ with the addition of GA' to the three lipid systems studied parallels the chain length dependence observed for $\Delta\nu_Q$. The largest change in cooperative length is observed for the system in which hydrophobic mismatch is the most severe. Thus, hydrophobic mismatch, which results in an extension of the lipid hydrocarbon chains, also decreases the cooperative length of the director fluctuations.

*The Bilayer to Hexagonal Transition in GA'/Lecithin Systems.* In order to understand the propensity of the GA'/lecithin systems to transform from the bilayer to $H_{II}$ phase, we draw an analogy to two geometrically similar transitions. The first is the transition from the micellar phase to the bilayer phase observed in GA'/lysopalmitoyllecithin (LPL) (Pasquali-Ronchetti et al., 1983; Killian et al., 1983; Killian & De Kruijff 1986), and the other, the transition from the bilayer phase to $H_{II}$ phase observed in palmitic acid (PA)/DPL at pH 4.0 (Marsh & Seddon, 1982).

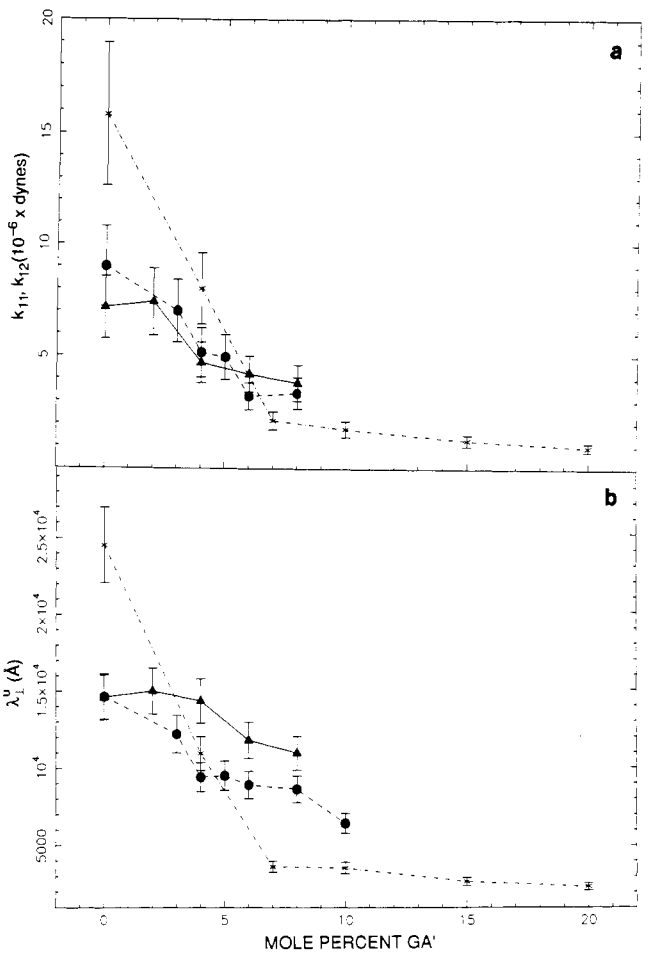


FIGURE 7: The model for cooperative director fluctuations in bilayers is used to extract both the elastic constant and the cooperative length of director fluctuations from the $T_1^{-1}$ and $T_2^{-1}$ measurements. (a) The elastic constant $(k_{11}, k_{22})$ is plotted versus GA' concentration for GA' in DML (×), DPL (●), and DSL (▲) bilayers. (b) The cooperative length, $\lambda_\perp^u$, is plotted as a function of GA' concentration in DML, DPL, and DSL bilayers. Symbols identifying each of the lipid systems are the same as in (a).

The headgroup area of pure LPL is much greater than the hydrocarbon area. Pure LPL in aqueous solution, therefore, self-assembles by forming micelles. When a sufficient amount of GA' is mixed with LPL, however, the bilayer phase is formed. Similarly, pure DPL in aqueous solution exists in the bilayer phase over a wide temperature range. However, when palmitic acid is added to DPL in a 3:2 molar ratio at pH 4.0, a bilayer → $H_{II}$ transition is induced at higher temperatures. A study of the temperature dependence of the bilayer → $H_{II}$ transition shows a direct transformation from the bilayer gel state to the $H_{II}$ phase. The bilayer liquid-crystalline state is bypassed completely. Based on $^{31}P$ NMR variable-temperature measurements, this phase is also bypassed in the GA'/DPL bilayer → $H_{II}$ transition.

In the GA'/LPL and PA/DPL systems, the GA' or PA molecules add to the hydrophobic area of the existing lipid structures. As the ratio of the hydrophobic area ($A_C$) to the headgroup area ($A_H$) (i.e., $A_C/A_H$) increases, a phase change is induced. In both cases, the new phase adopted is better able to accommodate the larger value of $A_C/A_H$. By analogy to the transitions described above, GA' induces a transition from bilayer → $H_{II}$ phase by increasing the ratio $A_C/A_H$ beyond a critical value.

There are three characteristics of the phase transitions in the GA′/lecithin systems that are worthy of note. Here, the transition is chain length dependent. The transition occurs most readily in lipid bilayers whose hydrophobic lengths nearly match or exceed that of GA′. The transition is not observed in DML, whose hydrophobic length is much less than that of GA′.

In addition, both the $T_{1\rho}^{-1}$ and $T_2^{-1}$ of deuterons at the 9- and 10-positions of DPL and DSL increase drastically and abruptly when GA′ is added to the $H_{II}$ phase, while the $^{31}P$ NMR spectra of the phospholipid headgroups in $H_{II}$ phase indicate little change in $T_2^{-1}$ upon addition of GA′. In $H_{II}$ phase, therefore, GA′ interferes significantly with chain motion but appears to have little effect on the motion of the lipid headgroups.

Lastly, in GA′/dioleoyllecithin bilayers, De Kruijff and co-workers have observed a reversion to bilayer phase at low water contents (Killian & De Kruijff, 1985). Although this phenomenon has been observed in other systems, it is contrary to lipid systems such as phosphatidylethanolamine (PE) which favor the $H_{II}$ phase at low water contents.

A simple geometric model proposed by Kirk et al. may be invoked to understand the characteristics of the bilayer → $H_{II}$ transition in GA′/lecithin systems under discussion here (Kirk et al., 1984; Kirk & Gruner, 1985; Gruner, 1985). In this model, a lipid system is characterized by an intrinsic radius of curvature ($R_0$). $R_0$ describes the curvature of the surface created by the lipid headgroups in the minimum-energy configuration. In the bilayer, $R_0$ is infinite. As the ratio $A_C/A_H$ increases, $R_0$ must decrease to accommodate the lipid in the aggregate structure. When $R_0$ is sufficiently small, the $H_{II}$ phase is formed. This model suggests that the addition of GA′ to lecithin bilayers increases $A_C/A_H$. At 6 mol % GA′, the $R_0$ of the DSL lipid system must have decreased sufficiently to accommodate the $H_{II}$ phase. For the DPL lipid system, 10 mol % GA′ is necessary to induce the $H_{II}$ phase. In the DML bilayer, however, no concentration of GA′ decreases $R_0$ sufficiently to stabilize the $H_{II}$ phase.

DML does not undergo the transition to $H_{II}$ phase upon addition of GA′. $A_C/A_H$, therefore, must not increase sufficiently to induce the $H_{II}$ phase in this system. If the DML hydrocarbon chain is not able to stretch sufficiently to contain the GA′ molecule in the hydrocarbon region of the bilayer, the GA′ molecule may protrude into the headgroup region of the bilayer. In this case, an increase in the hydrophobic area of the bilayer is counteracted to some extent by a similar increase in the headgroup area. Thus, both $A_C/A_H$ and $R_0$ change less in DML than in DPL and DSL, and the $H_{II}$ phase is never stabilized.

Finally, to understand the inhibition of $H_{II}$ phase by low water contents, consider the aqueous inner tube of the $H_{II}$ cylinder which must be completely filled with water. As the water content is decreased, the radius of this inner tube must shrink. In excess water, high concentrations of GA′ alter the $R_0$ of DPL and DSL bilayers sufficiently to induce $H_{II}$ phase in excess water. At very low water contents, however, the water present may only be sufficient to fill a narrow $H_{II}$ cylinder. If the radius of this cylinder is much smaller than $R_0$, then only the bilayer phase will be energetically accessible to the GA′/lipid system.

## Acknowledgments

Access to the Southern California Regional NMR Facility at Caltech, supported by National Science Foundation Grant CHE84-40137, for the NMR experiments is gratefully acknowledged. We thank Drs. T. Handel, A. Nayeem, H. Eckert, and J. Yesinowski for helpful discussions and assistance.

## References

Aslanian, D., Negrerie, M., & Chambert, R. (1986) *Eur. J. Biochem. 160*, 395–400.
Chapman, D., Cornell, B. A., Eliasz, A. W., & Perry, A. (1977) *J. Mol. Biol. 113*, 517–538.
Chupin, V., Killian, J. A., & De Kruijff, B. (1987) *Biophys. J. 51*, 394–405.
Cornell, B. A., & Separovic, F. (1988) *Eur. Biophys. J. 16*, 299–306.
Cornell, B. A., Separovic, A. J., Baldassi, A. J., & Smith, R. (1988a) *Biophys. J. 53*, 67–76.
Cornell, B. A., Weir, L. E., & Separovic, F. (1988b) *Eur. Biophys. J. 16*, 113–119.
Fisher, R., & Blumenthal, T. (1982) *Proc. Natl. Acad. Sci. U.S.A. 79*, 1045–1048.
Gruner, S. M. (1985) *Proc. Natl. Acad. Sci. U.S.A. 82*, 3665–3669.
Iqbal, Z., & Weidekamm, E. (1980) *Arch. Biochem. Biophys. 202*, 639–649.
Killian, J. A., & De Kruijff, B. (1985) *Biochemistry 24*, 7890–7898.
Killian, J. A., & De Kruijff, B. (1986) *Chem. Phys. Lipids 40*, 259–284.
Killian, J. A., & De Kruijff, B. (1988) *Biophys. J. 53*, 111–117.
Killian, J. A., De Kruijff, B., Van Echteld, C. J. A., Verkleij, A. J., Leunissen-Bijvelt, J., & De Gier, J. (1983) *Biochim. Biophys. Acta 728*, 141–144.
Killian, J. A., Van den Berg, C. W., Tournois, H., Keur, S., Slotboom, A. J., Van Scharrenburg, G. J. M., & de Kruijff, B. (1986) *Biochim. Biophys. Acta 857*, 13–27.
Killian, J. A., Prasad, K. U., Urry, D. W., & De Kruijff, B. (1989) *Biochim. Biophys. Acta 978*, 341–345.
Kirk, G. L., & Gruner, S. M. (1985) *J. Phys. (Paris) 46*, 761–769.
Kirk, G. L., Gruner, S. M., & Stein, D. L. (1984) *Biochemistry 23*, 1093–1102.
Kusumi, A., & Hyde, J. S. (1982) *Biochemistry 21*, 5978–5983.
Lee, D. C., Durrani, A. A., & Chapman, D. (1984) *Biochim. Biophys. Acta 769*, 49–56.
Lewis, B. A., & Engelman, D. M. (1983) *J. Mol. Biol. 166*, 203–210.
Marsh, D., & Seddon, J. M. (1982) *Biochim. Biophys. Acta 690*, 117–123.
Naik, V. M., & Krimm, S. (1984) *Biophys. J. 45*, 109–112.
Naik, V. M., & Krimm, S. (1986) *Biophys. J. 49*, 1147–1154.
Pace, R. J., & Chan, S. I. (1982a) *J. Chem. Phys. 76*, 4217–4227.
Pace, R. J., & Chan, S. I. (1982b) *J. Chem. Phys. 76*, 4228–4240.
Pasquali-Ronchetti, I., Spisni, A., Casali, E., Masotti, L., & Urry, D. W. (1983) *Biosci. Rep. 3*, 127–133.
Pearson, L. T., Chan, S. I., Lewis, B. A., & Engelman, D. M. (1983) *Biophys. J. 43*, 167–174.
Pearson, L. T., Edelman, J., & Chan, S. I. (1984) *Biophys. J. 45*, 863–871.
Rice, D., & Oldfield, E. (1979) *Biochemistry 18*, 3272–3279.
Riegler, J., & Moehwald, H. (1986) *Biophys. J. 49*, 1111–1118.
Seelig, J. (1977) *Q. Rev. Biophys. 10*, 353–418.
Urry, D. W., Goodall, M. C., Glickson, J. D., & Mayers, D. F. (1971) *Proc. Natl. Acad. Sci. U.S.A. 68*, 1907–1911.

Urry, D. W., Trapane, J. U., & Prasad, K. U. (1983) *Science 221*, 1064–1067.
Van Echteld, C. J. A., De Kruijff, B., Verkleij, A. J., Leunissen-Bijvelt, J., & De Gier, J. (1982) *Biochim. Biophys. Acta 692*, 126–138.
Veatch, W. R., Fossel, E. T., & Blout, E. R. (1974) *Biochemistry 13*, 5249–5256.
Watnick, P. I., Dea, P., Nayeem, A., & Chan, S. I. (1987) *J. Chem. Phys. 86*, 5789–5800.
Watnick, P. I., Dea, P., & Chan, S. I. (1990) *Proc. Natl. Acad. Sci. U.S.A. 87*, 2082–2086.
Weinstein, S., Wallace, B. A., Blout, E. R., Morrow, J., & Veatch, W. (1979) *Proc. Natl. Acad. Sci. U.S.A. 76*, 4230–4234.
Weinstein, S., Wallace, B. A., Morrow, J., & Veatch, W. (1980) *J. Mol. Biol. 143*, 1–19.

# Mapping of a Cholinergic Binding Site by Means of Synthetic Peptides, Monoclonal Antibodies, and α-Bungarotoxin†

Bianca M. Conti-Tronconi,*,‡ Fen Tang,‡ Brenda M. Diethelm,‡ Sandra R. Spencer,‡ Sigrid Reinhardt-Maelicke,§ and Alfred Maelicke§

*Department of Biochemistry, College of Biological Sciences, University of Minnesota, 1479 Gortner Avenue, St. Paul, Minnesota 55108, and Max-Planck-Institut fur Ernahrungsphysiologie, 201 Rheinlanddamm, D-4600 Dortmund, West Germany*

*Received August 31, 1989; Revised Manuscript Received January 29, 1990*

ABSTRACT: Previous studies by several laboratories have identified a narrow sequence region of the nicotinic acetylcholine receptor (AChR) α subunit, flanking the cysteinyl residues at positions 192 and 193, as containing major elements of, if not all, the binding site for cholinergic ligands. In the present study, we used a panel of synthetic peptides as representative structural elements of the AChR to investigate whether additional segments of the AChR sequences are able to bind α-bungarotoxin (α-BTX) and several α-BTX-competitive monoclonal antibodies (mAbs). The mAbs used (WF6, WF5, and W2) were raised against native *Torpedo* AChR, specifically recognize the α subunit, and bind to AChR in a mutually exclusive fashion with α-BTX. The binding of WF5 and W2 to *Torpedo* AChR is inhibited by all cholinergic ligands. WF6 competes with agonists, but not with low mol. wt. antagonists, for AChR binding. The synthetic peptides used in this study were approximately 20 residue long, overlapped each other by 4–6 residues, and corresponded to the complete sequence of *Torpedo* AChR α subunit. Also, overlapping peptides, corresponding to the sequence segments of each *Torpedo* AChR subunit homologous to α166–203, were synthesized. α-BTX bound to a peptide containing the sequence α181–200 and also, albeit to a lesser extent, to a peptide containing the sequence α55–74. WF6 bound to α181–200 and to a lesser extent to α55–74 and α134–153. The two other mAbs predominantly bound to α55–74, and to a lesser extent to α181–200. Peptides α181–200 and α55–74 both inhibited binding of $^{125}$I-α-BTX to native *Torpedo* AChR. None of the peptides corresponding to sequence segments from other subunits bound α-BTX or WF6, or interfered with their binding. Therefore, the cholinergic binding site is not a single narrow sequence region, but rather two or more discontinuous sequence segments within the N-terminal extracellular region of the AChR α subunit, folded together in the native structure of the receptor, contribute to form a cholinergic binding region. Such a structural arrangement is similar to the "discontinuous epitopes" observed by X-ray diffraction studies of antibody–antigen complexes [reviewed in Davies et al. (1988)].

The nicotinic acetylcholine receptors (AChRs)[1] are complex transmembrane proteins formed by homologous subunits [reviewed in McCarthy et al. (1986), Maelicke (1988), and Lindstrom et al. (1987)] which in peripheral tissues, such as fish electroplax and skeletal muscle, are assembled in a stoichiometry of $\alpha_2\beta\gamma\delta$ (Raftery et al., 1980; Conti-Tronconi et al., 1982). The AChR subunits are structurally related, suggesting that they have evolved from a common ancestor (Raftery et al., (1980), and they form a family of proteins with other ligand-gated ion channels, such as the glycine and the $GABA_A$ receptors, in spite of the fact that the latter are selective for the anion chloride rather than cations like the AChR (Grenningloh et al., 1987; Levitan et al., 1988). Elucidation

†Supported by NSF Grant BNS-8607289 (to B.M.C.-T.), NINCDS Grant NS 29919 (to B.M.C.-T.), ARO Contract DAMD 17-88-C-8120 (to B.M.C.-T.), Deutsche Forshungsgemeinschaft Grants SFB 168-B2 and Ma 599/10-1 (to. A.M.), and a Fonds der Chemischen Industrie Grant (to A.M.).

*To whom correspondence should be addressed.
‡University of Minnesota.
§Max-Planck-Institut fur Ernahrungsphysiologie.

[1] Abbreviations: AChR, nicotinic acetylcholine receptor; α-BTX, α-bungarotoxin; α-CTX, α-cobratoxin, α-naja toxin; mAb, monoclonal antibody; IgG, immunoglobulin G; Ag, antigen; MIR, main immunogenic region; ELISA, enzyme-linked immunosorbent asay; SPRIA, solid-phase radioimmunoassay; HPLC, high-pressure liquid chromatography; MBTA, [4-(*N*-maleimido)benzyl]trimethylammonium; DDF, *p*-(dimethylamino)benzenediazonium fluoroborate; Tris, tris(hydroxymethyl)aminomethane; BSA, bovine serum albumin; Prot A, protein A; TBS, 10 mM Tris buffer, pH 7.4, containing 140 mM NaCl; TBS–Tween, 10 mM Tris buffer, pH 7.4, containing 140 mM NaCl and 0.1% Tween; HST, 10 mM Tris-HCl buffer, pH 7.4, containing 500 mM NaCl and 0.5% Tween; PBS, 10 mM sodium phosphate buffer, pH 7.4, containing 140 mM NaCl; PBS–Tween, 10 mM sodium phosphate buffer, pH 7.4, containing 140 mM NaCl and 0.05% Tween-20; PBS–BSA, 10 mM sodium phosphate buffer, pH 7.4, containing 140 mM NaCl and 0.4% BSA.

0006-2960/90/0429-6221$02.50/0 